Research Square

Preprints are preliminary reports that have not undergone peer review.
They should not be considered conclusive, used to inform clinical practice,
or referenced by the media as validated information.

# High expression of fibroblast activation protein in hepatocellular carcinoma: characteristics of angiogenesis and immune infiltration

**Ze-Jie Sang**
The Fourth Medical Center of PLA General Hospital
**Yan Bao**
The Second Xiangya Hospital of Central South University
**Wei-Qian Lu**
7716453840qq.com

Hunan Provincial of Integrated Traditional Chinese and Western Medicine

**Research Article**

**Keywords:** Fibroblast activation protein, Hepatocellular carcinoma, Angiogenesis, immune infiltration, Vessels encapsulating tumor clusters (VETC), Tertiary lymphoid structures (TLS)

**Posted Date:** July 10th, 2026

**DOI:** https://doi.org/10.21203/rs.3.rs-10263603/v1

**License:** This work is licensed under a Creative Commons Attribution 4.0 International License.
Read Full License

**Additional Declarations:** No competing interests reported.

**Title**: High expression of fibroblast activation protein in hepatocellular carcinoma: characteristics of angiogenesis and immune infiltration

Ze-Jie Sang[2], Yan Bao[3], Wei-Qian Lu[1*]

Affiliations:

1 Department of Pathology, Hunan Provincial of Integrated Traditional Chinese and Western Medicine, Changsha, 410006, Hunan Province, China

2 Department of Interventional Radiology, the Fourth Medical Center of PLA General Hospital, Beijing, 100037, China

3 Department of Radiology, the Second Xiangya Hospital of Central South University, Changsha, 410011, Hunan Province, China

Corresponding author: Dr. Wei-Qian Lu, Department of Pathology, Hunan Provincial of Integrated Traditional Chinese and Western Medicine, No. 58 Lushan Road, Changsha, 410006, Hunan Province, China (E-mail: 771645384@qq.com)

**Abstract**

**Background**: The tumor microenvironment (TME) plays a critical role in the progression of hepatocellular carcinoma (HCC) and is associated with angiogenesis and antitumor immunity. Fibroblast activation protein (FAP) positive cancer-associated fibroblasts (CAFs) are important stromal components of the TME; however, their relationship with distinct vascular patterns, particularly vessels encapsulating tumor clusters (VETC) and tertiary lymphoid structures (TLS) remains poorly characterized.

**Materials and methods**: This multicenter study included a retrospective cohort of 1003 patients with HCC who underwent curative resection between January 2014 and June 2022 and a prospective genomic cohort of 23 patients enrolled between March 2024 and November 2025. FAP expression was evaluated using the H-score, and patients were classified into low- and high-FAP groups.

Differences in microvascular density (MVD), VETC patterns, and TLSs were compared between the groups. Overall survival (OS) and recurrence-free survival (RFS) were analyzed using log-rank tests before and after propensity score matching (PSM) and inverse probability of treatment weighting (IPTW). Single-cell RNA sequencing (scRNA-seq) was used to explore angiogenic and immune-related signatures.

**Results**: Compared to low-FAP HCCs (n=777), high-FAP HCCs (n=226) exhibited a significantly higher prevalence of poor tumor differentiation (51.3% vs. 30.8%), VETC patterns (44.2% vs. 28.2%), and elevated MVD levels (all adjusted P<0.001), whereas the incidence of intratumoral TLSs was significantly lower (39.4% vs. 54.8%, adjusted P<0.001). These associations remained significant after PSM and IPTW analyses. Patients in the low-FAP group had significantly better OS and RFS than those in the high-FAP group before matching (P<0.001), after PSM (P=0.041 for OS; P=0.023 for RFS), and after IPTW (P=0.030 for OS; P=0.021 for RFS). scRNA-seq showed that high FAP expression was positively correlated with the proangiogenic marker *PDGFRB* (adjusted P<0.001), and with angiogenesis-related signaling pathways, such as VEGF, MAPK, and focal adhesion. Furthermore, high FAP expression was associated with a reduced proportions of CD8+ tissue-resident memory T cells (TRM) (adjusted P=0.044).

**Conclusions**: FAP expression is associated with a proangiogenic and immunosuppressive TME in HCC, characterized by the enrichment of VETC vascular patterns and reduced TLS formation. These findings suggest that FAP-positive CAFs may contribute to the spatial organization of tumor vasculature and immune exclusion, supporting further evaluation of FAP as a potential biomarker and therapeutic target in HCC.

**Keywords:** Fibroblast activation protein; Hepatocellular carcinoma; Angiogenesis; immune infiltration; Vessels encapsulating tumor clusters (VETC); Tertiary lymphoid structures (TLS)

## 1. Introduction

Hepatocellular carcinoma (HCC) is the most common primary liver malignancy and a leading

cause of cancer-related mortality worldwide [1,2]. Despite advances in surgical resection and systemic therapies, the long-term prognosis of patients with HCC remains unsatisfactory due to high rates of recurrence and metastasis [3,4]. Increasing evidence indicates that tumor progression depends not only on genetic alterations within malignant hepatocytes, but also on interactions within the tumor microenvironment (TME), which regulates angiogenesis, immune surveillance, and metastatic dissemination [5,6].

Among the stromal components of the TME, cancer-associated fibroblasts (CAFs) have emerged as important contributors to tumor progression [7]. Fibroblast activation protein (FAP), a type II transmembrane serine protease selectively expressed by activated fibroblasts, is one of the recognized markers of CAFs [8]. Previous studies have demonstrated that FAP-positive CAFs promote tumor growth, angiogenesis, and immune evasion in multiple malignancies [9,10]. Although FAP-positive CAFs are known to influence the TME through extracellular matrix (ECM) remodeling and the secretion of growth factors, their potential role in coordinating the higher-order structural organization of the HCC TME remains poorly characterized.

Two critical structural features that influence HCC progression are vascular architecture and the organization of the immune microenvironment. The vessels-encapsulating tumor clusters (VETC) pattern is a distinctive vascular phenotype that may promote tumor growth and facilitates metastasis [11-13]. Tertiary lymphoid structures (TLS) are ectopic lymphoid aggregates that foster robust antitumor immunity and are associated with favorable clinical outcomes [14-15]. Through ECM remodeling and the secretion of proangiogenic factors such as VEGF, CAFs may facilitate VETC formation [16]. Meanwhile, CAF-derived matrix components and immunomodulatory cytokines, including TGF-$\beta$, may create physical and biochemical barriers that restrict lymphocyte infiltration and impair TLS assembly [15,17]. Accordingly, it is hypothesized that FAP-positive CAFs may contribute to shaping these divergent TME patterns. However, the associations between FAP expression, coordinated vascular remodeling, and immune exclusion in HCC remains unclear.

In this study, we investigated the relationship between FAP expression, angiogenic patterns, and

immune organization in HCC. By integrating a large multicenter cohort with single-cell transcriptomic analysis, we examined whether FAP expression is associated with vascular remodeling and immune infiltration within the TME.

## 2. Materials and Methods

*Study patients*

This multicenter study included one retrospective dataset and one prospective dataset from three tertiary referral hospitals and was conducted in accordance with the Declaration of Helsinki. The study protocol was approved by the institutional review boards of all participating hospitals. Written informed consent was obtained from patients in the prospective cohort, whereas the requirement for informed consent was waived for the retrospective cohort owing to its retrospective design.

This retrospective cohort included 1003 consecutive adult patients with untreated HCC who underwent liver resection (LRE) at three institutions between January 2014 and June 2022. All patients were successfully target-tested for histopathological evaluation. Specifically, 500 patients were enrolled at the Second Xiangya Hospital of Central South University (January 2014 to May 2022), 302 at the Fourth Medical Center of PLA General Hospital (March 2015 to June 2022), and 201 at the Hunan Provincial Hospital of Integrated Traditional Chinese and Western Medicine (February 2016 to December 2021). A prospective genomic cohort comprising consecutive adult patients with untreated HCC who underwent LRE at the Second Xiangya Hospital of Central South University between March 2024 and November 2025 was also recruited. The inclusion criteria for all cohorts were as follows: (1) preserved liver function, (2) an Eastern Cooperative Oncology Group performance status of 0, and (3) absence of macrovascular invasion or extrahepatic metastasis. The exclusion criteria for the retrospective cohort were as follows: (1) noncurative resection with R1 or R2 margins, (2) absence of baseline laboratory information within 1 week before LRE, (3) unavailability of pathology slides for histological staining, and (4) loss to follow-up. The exclusion criterion for the genomic test cohort was an unqualified single-cell suspension for sequencing. A flowchart of the study design is shown in Figure 1.

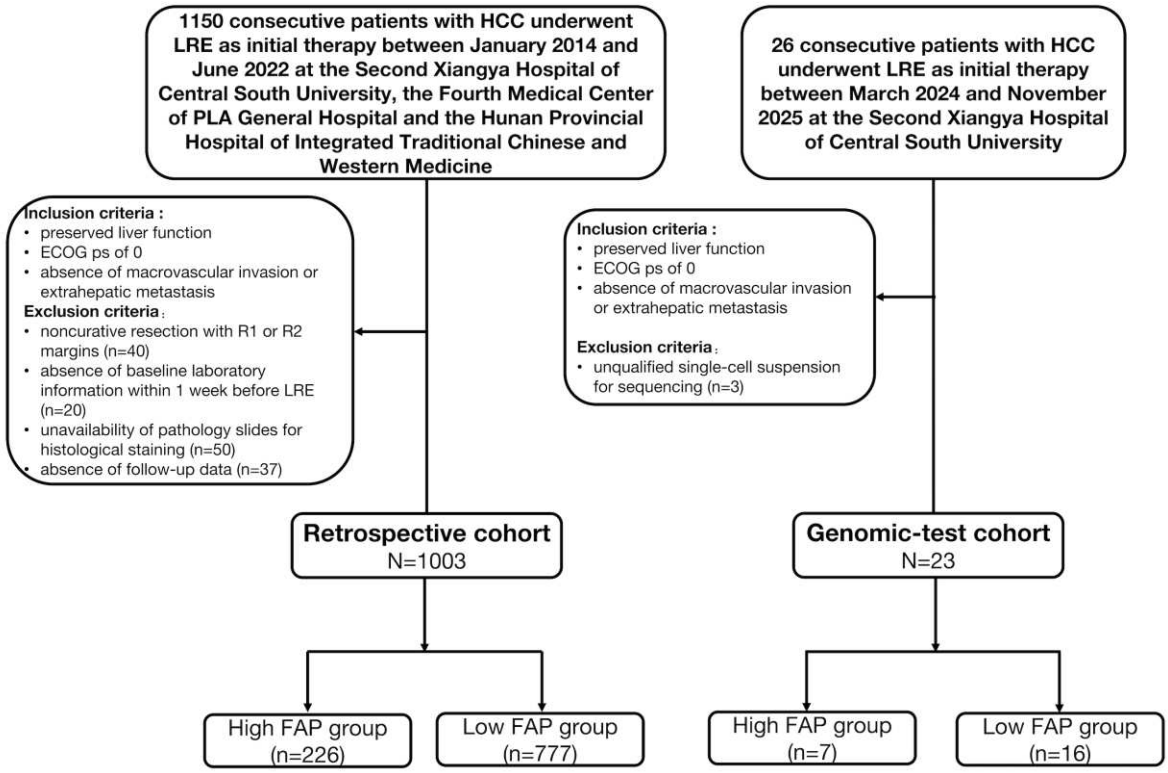



Figure 1. Flowchart of the study population.

*Clinical data and follow-up*

Baseline clinical data including age, sex, Barcelona Clinic Liver Cancer stage, liver cirrhosis status, and the etiology of the underlying liver disease were collected. Laboratory data, including neutrophil,

lymphocyte, monocyte, and platelet counts, as well as serum albumin, total bilirubin, alanine aminotransferase, aspartate aminotransferase, international normalized ratio (INR), creatinine, and alpha-fetoprotein (AFP) levels, were also collected.

Patients were monitored for 2-3 months after LRE and at least every 6 months thereafter. Surveillance for tumor recurrence routinely involved contrast-enhanced computed tomography (CT) or magnetic resonance imaging (MRI), along with serum AFP measurements. Follow-up data were updated through December 2025 via telephone interviews or through review of the most recent clinical records when telephone contact was unavailable. The primary clinical outcome was overall survival (OS), defined as the interval from LRE to death from any cause. The secondary outcome was recurrence-free survival (RFS), defined as the interval from LRE to tumor recurrence.

*Histological examination*

Diagnostic and morphological evaluations were conducted independently by two hepatopathologists with 11 and 13 years of expertise, respectively, and any interpretive discrepancies were resolved by collaborative consensus. All HCC cases were staged and diagnosed according to the 2019 WHO classification [18]. To evaluate FAP expression, archival formalin-fixed, paraffin-embedded (FFPE) tissue blocks for all 1,003 patients were retrieved from the respective pathology departments. For immunohistochemical analysis, 5-μm FFPE tissue sections were subjected to a standardized protocol, including rehydration and microwave-assisted antigen retrieval. These sections were subsequently incubated overnight at 4°C with monoclonal primary antibodies against human CD34 and FAP (Supplementary Table S1). Following a 30-minute incubation with secondary antibodies at 37 ℃, signals were developed using avidin-horseradish peroxidase (25 min) and 3,3’-diaminobenzidine (5 min) for visualization.

FAP expression was quantified using the H-score method, defined as the mathematical product of staining intensity (graded semiquantitatively from 0 [negative] to 3 [intense]) and the respective percentage of positive neoplastic and stromal cells. Consistent with established protocols, an H-score

threshold of 10 was used to stratify patients into low-FAP (H-score ≤10) and high-FAP (H-score >10) cohorts (Figure 2) [19].

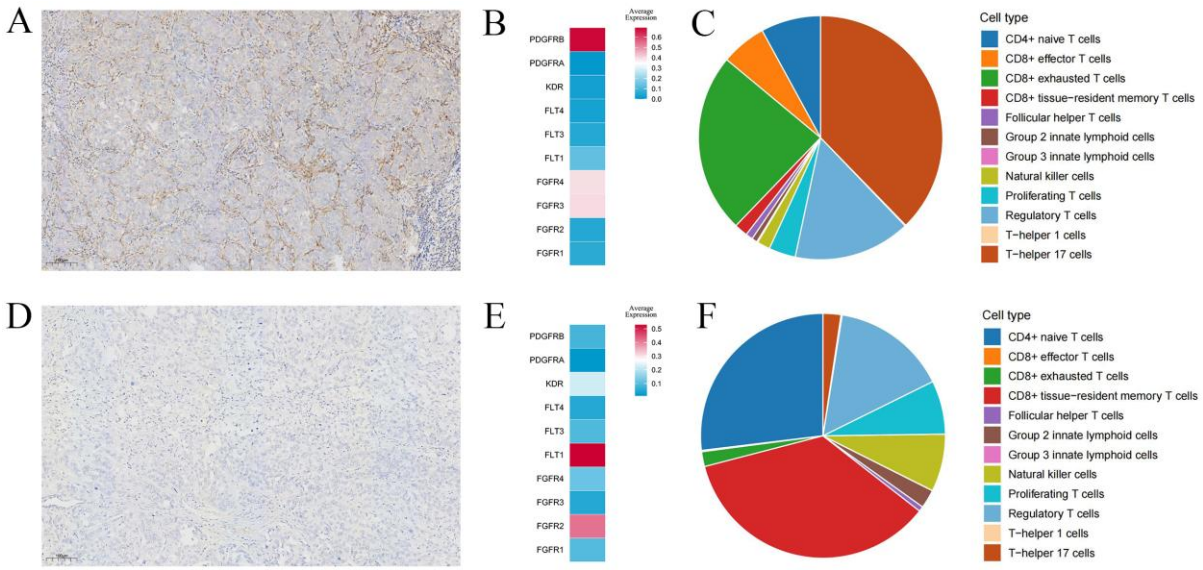



Figure 2. Integrated characterization of the tumor microenvironment in representative HCC patients with high and low FAP expression.

(A-C) A representative case of high FAP expression in a 61-year-old male with chronic hepatitis B virus (HBV)-related HCC and high FAP expression. (A) Immunohistochemistry (IHC) staining shows intense and diffuse FAP expression within the tumor stroma. (B) scRNA-seq profile shows markedly elevated transcript levels of pro-angiogenic genes, particularly PDGFRB. (C) The pie chart displaying this high-FAP case is consistent with an immunosuppressive landscape characterized by a sparse population of CD8+ tissue-resident memory T cells (TRM). (D-F) A representative case of low FAP expression in a 51-year-old female with chronic HBV-related HCC and low FAP expression. (D) IHC staining shows low FAP expression in the intratumoral stroma. (E) scRNA-seq analysis shows significantly lower PDGFRB levels. (F) A pie chart showing this low-FAP case has a higher percentage of CD8+ TRM cells. FAP, fibroblast activation protein; HCC, hepatocellular carcinoma

MVD was assessed by identifying three vascular "hot-spots" at 100x magnification, followed by definitive vessel counting at 200x magnification. The final MVD value represents the mean count across these three fields. VETC, characterized by CD34-positive sinusoidal structures surrounding discrete tumor nests in a cobweb-like configuration, was considered positive when the VETC pattern involved $\geq$5% of the total tumor area [11].

Morphological evaluation of intratumoral TLS in tumors was performed using Hematoxylin and Eosin (H&E)-stained slides [14]. TLS were classified as follows : 1) aggregates, defined as vague, ill-defined clusters of lymphocytes; 2) primary follicles, defined as round clusters of lymphocytes without germinal center formation; and 3) secondary follicles, defined as follicles with germinal center formation. Tumors containing at least one TLS were classified as TLS+, whereas tumors without any TLSs were classified as TLS-. A schematic illustration of these pathological indicators is shown in Figure 3.

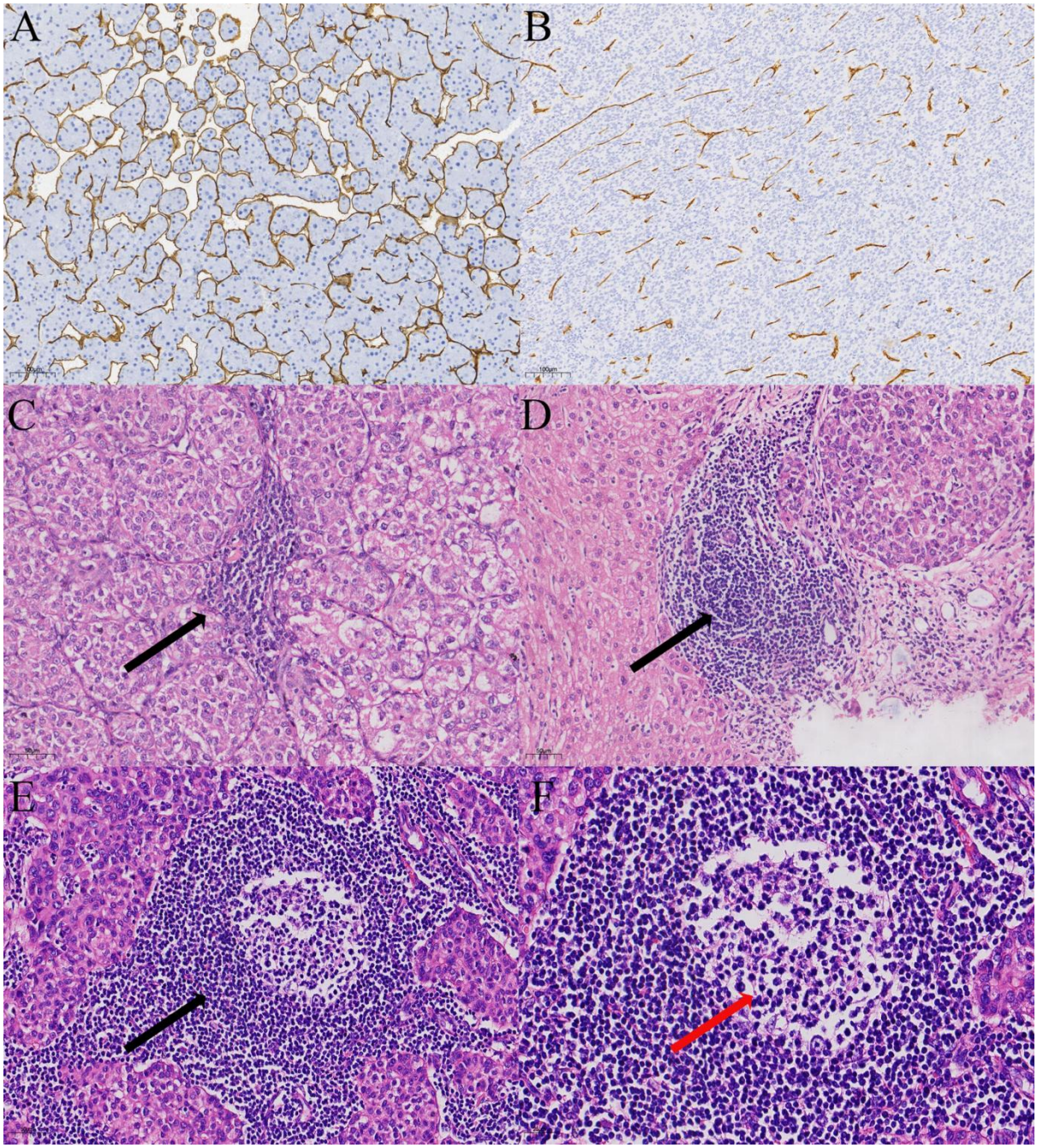



Figure 3. Histological features of the VETC patterns and intratumoral TLS. (A) VETC-positive (VETC+): CD34 immunohistochemical staining highlights a "vessels encapsulating tumor clusters" pattern, characterized by endothelium-lined vessels surrounding discrete tumor nests (CD34, X100). (B) VETC-negative (VETC-): CD34 staining shows a conventional sinusoidal or disorganized angiogenesis pattern, in which the vessels do not encapsulate tumor clusters (CD34, X100). (C) Lymphocyte aggregates: Vague and ill-defined clusters of lymphocytes (black arrow, HE, X200). (D) Primary follicles: Dense, round or oval-shaped clusters of lymphocytes without a germinal center (black

arrow, HE, X200). (E) Secondary follicles: Organized lymphoid structures centered by a distinct germinal center (black arrow, HE, X200). (F) Secondary follicle at high magnification: Microscopic examination shows a pale central area (germinal center, red arrow) surrounded by a dense outer rim of small lymphocytes (mantle zone) (HE, X400). VETC, vessels encapsulated tumor clusters

*Angiogenesis and immune infiltration levels analyses*

Patients in the genomic cohort were categorized into low- and high-FAP groups. Single-cell RNA sequencing (scRNA-seq; Supplementary Material) was used to compare the expression of angiogenesis-related genes [20] (e.g., *KDR*, *FGFR,* and *PDGFR*) and the distribution of immune cell populations between the two groups. Cell type identification for each cluster was performed using canonical markers, genes obtained from the SynEcoSys™ reference database (Singleron Biotechnology). Significant differences in gene expression and cell-type distribution were identified, with P-values adjusted using the Benjamini-Hochberg correction. Furthermore, Gene Set Enrichment Analysis (GSEA) was used to identify potential signaling pathways associated with the observed angiogenic signatures.

*Statistical analyses*

Categorical variables were compared via the $\chi^2$ test or Fisher's exact test, whereas continuous variables were compared via the Mann–Whitney U test or Student's t test, depending on their distribution. To control the false discovery rate (FDR) across multiple baseline comparisons, P-values for baseline clinical characteristics were further adjusted using the Benjamini-Hochberg method. Interreader agreement for histological characteristics was assessed using the kappa coefficient

(Supplementary Material). RFS and OS were compared using the log-rank test. Furthermore, multivariable Cox proportional hazards regression analysis was performed on the entire cohort to identify independent prognostic predictors of RFS and OS, while simultaneously adjusting for potential clinical and pathological confounders. To equilibrate the distribution of baseline covariates between the study groups and minimize inherent selection bias, a comprehensive strategy involving Propensity Score Matching (PSM) and weighting was employed. Specifically, a 1:1 nearest-neighbor PSM protocol was implemented based on logit-transformed propensity scores, with a matching caliper strictly limited to 0.1 to ensure precise pair alignment. To further validate the robustness of the findings, stabilized inverse probability of treatment weighting (IPTW) was applied. This dual approach generated a weighted pseudo-cohort in which baseline patient characteristics were balanced between the high- and low-FAP cohorts without artificially inflating the total sample size .

The required sample size was determined via power calculations (Supplementary Material). R software, version 4.0.2 (R Foundation for Statistical Computing; http://www.R-project.org), G*Power software (https://stats.oarc.ucla.edu/other/gpower), and SPSS, version 29.0 (IBM) were used to perform the statistical analyses. Statistical significance was defined as a two-sided p-value <0.05.

## 3. Results

*Baseline patient characteristics*

In the retrospective cohort, 1150 patients were initially included, of whom 147 were excluded. The final study population comprised 1003 patients (842 men and 161 women; mean age, 53.7 ± 11.8 years). In total, 226 HCC samples were classified as having high FAP expression, whereas 777 were classified as having low FAP expression. The median follow-up time was 49.0 months (interquartile range [IQR], 27.5-71.9 months). Compared with patients with low FAP expression, patients with high FAP expression were more likely to have serum alpha fetoprotein levels higher than 200 ng/mL (102 out of 226 cases [45.1%] vs 288 out of 777 cases [37.1%]); P=0.035, adjusted P=0.129), tumor size greater than 5 cm (128 out of 226 cases [56.6%] vs 346 out of 777 cases [44.5%]); P=0.002, adjusted

P=0.009) and higher neutrophil count(3.54, IQR: 2.44-4.64 vs. 3.24, IQR: 2.38-4.22; P=0.027, adjusted P=0.115). The baseline information of the study population is presented in Table 1. The study flowchart is shown in Figure 1.

Table1. Baseline clinical and pathologic characteristics of patients in total cohorts

| Baseline characteristics | Retrospective cohort (n=1003) | Low FAP group (n=777) | High FAP group (n=226) | *P* | *Adjusted P* ^ | Genomic-test cohort (n=23) |
|---|---|---|---|---|---|---|
| Age (years) * | 53.7±11.8 | 53.8±12.0 | 53.4±11.5 | 0.594 | 0.736 | 58.1±9.0 |
| Gender (N, %) | | | | 0.873 | 0.897 | |
| male | 842 (83.9) | 651 (83.8) | 191 (84.5) | | | 18 (78.3) |
| female | 161 (16.1) | 126 (16.2) | 35 (15.5) | | | 5 (21.7) |
| Underlying liver diseases (N, %) | | | | 0.328 | 0.502 | |
| absence | 131 (13.1) | 106 (13.6) | 25 (11.1) | | | 4 (17.4) |
| HBV | 785 (78.3) | 600 (77.2) | 185 (81.9) | | | 14 (60.9) |
| others | 87 (8.7) | 71 (9.1) | 16 (7.1) | | | 5 (21.7) |
| Liver cirrhosis (N, %) | | | | 0.636 | 0.739 | |
| absence | 512 (51.0) | 393 (50.6) | 119 (52.7) | | | 5 (21.7) |
| presence | 491 (49.0) | 384 (49.4) | 107 (47.3) | | | 18 (78.3) |
| Ascites (N, %) | | | | 0.654 | 0.739 | |
| absence | 918 (91.5) | 709 (91.2) | 209 (92.5) | | | 22 (95.7) |
| little | 85 (8.5) | 68 (8.8) | 17 (7.5) | | | 1 (4.3) |

| | | | | | | | | | | | | |
|---|---|---|---|---|---|---|---|---|---|---|---|---|
| Neutrophil (×$10^9$) # | 3.30 | (2.39-4.30) | 3.24 | (2.38-4.22) | 3.54 | (2.44-4.64) | 0.027 | 0.115 | 3.19 | (2.72, 3.54) |
| Lymphocyte (×$10^9$) # | 1.37 | (1.04-1.74) | 1.38 | (1.05-1.76) | 1.33 | (1.03-1.65) | 0.314 | 0.502 | 1.24 | (1.06-1.61) |
| Platelet (×$10^9$) # | 156 | (111-209) | 155 | (110-206) | 162 | (117-211) | 0.270 | 0.502 | 135 | (97-157) |
| Monocyte (×$10^9$) # | 0.34 | (0.25-0.46) | 0.34 | (0.25-0.45) | 0.36 | (0.25-0.47) | 0.297 | 0.502 | 0.35 | (0.29-0.38) |
| Albumin (g/L) # | 39.3 | (36.3-42.2) | 39.3 | (36.3-42.1) | 39.2 | (36.3-42.2) | 0.528 | 0.687 | 42.0 | (39.0-42.8) |
| Total bilirubin (umol/L) # | 13.7 | (10.3-18.2) | 13.9 | (10.4-17.9) | 13.4 | (9.9-19.0) | 0.852 | 0.897 | 13.7 | (11.5-25.8) |
| ALT (U/L) # | 31.0 | (21.1-47.3) | 31.4 | (21.6-47.5) | 29.5 | (19.8-45.7) | 0.086 | 0.281 | 31.0 | (24.2-43.1) |
| AST (U/L) # | 34.1 | (24.7-49.9) | 34.1 | (24.7-49.8) | 33.6 | (24.5-51.1) | 0.897 | 0.897 | 36.3 | (26.9-52.5) |
| Creatinine (umol/L) # | 71.2 | (61.0-80.6) | 71.6 | (61.8-80.8) | 70.1 | (59.6-79.9) | 0.355 | 0.513 | 72.6 | (64.5-87.0) |
| INR | 1.02 | (0.96-1.09) | 1.02 | (0.96-1.09) | 1.03 | (0.97-1.10) | 0.149 | 0.322 | 1.02 | (0.97-1.06) |
| ALBI grade (N, %) | | | | | | | 0.147 | 0.322 | | |
| I | 493 (49.2) | | 392 (50.5) | | 101 (44.7) | | | | 17 (73.9) | |
| II | 510 (50.8) | | 385 (49.5) | | 125 (55.3) | | | | 6 (26.1) | |
| AFP (ng/mL, N, %) | | | | | | | 0.035 | 0.129 | | |
| ≤200 | 613 (61.1) | | 489 (62.9) | | 124 | (54.9) | | | 15 (65.2) | |

| | | | | | | |
|---|---|---|---|---|---|---|
| >200 | 390 (38.9) | 288 (37.1) | 102 (45.1) | | | 8 (34.8) |
| Tumor size (mm, N, %) | | | | 0.002 | 0.009 | |
| ≤50 | 529 (52.7) | 431 (55.5) | 98 (43.4) | | | 11 (47.8) |
| >50 | 474 (47.3) | 346 (44.5) | 128 (56.6) | | | 12 (52.2) |
| Microvascular invasion (N, %) | | | | 0.466 | 0.687 | |
| absence | 545 (54.3) | 427 (55.0) | 118 (52.2) | | | 14 (60.9) |
| presence | 458 (45.7) | 350 (45.0) | 108 (47.8) | | | 9 (39.1) |
| Satellite lesions (N, %) | | | | 0.251 | 0.502 | |
| absence | 729 (72.7) | 572 (73.6) | 157 (69.5) | | | 19 (82.6) |
| presence | 274 (27.3) | 205 (26.4) | 69 (30.5) | | | 4 (17.4) |
| Tumor differentiation (N, %) | | | | <0.001 | <0.001 | |
| Moderately to well | 648 (64.6) | 538 (69.2) | 110 (48.7) | | | 16 (69.6) |
| poorly | 355 (35.4) | 239 (30.8) | 116 (51.3) | | | 7 (30.4) |
| Intratumoral TLS | | | | <0.001 | <0.001 | |
| absence | 488 (48.7) | 351 (45.2) | 137 (60.6) | | | 11 (47.8) |
| presence | 515 (51.3) | 426 (54.8) | 89 (39.4) | | | 12 (52.2) |
| MVD | 67.0 (41.7-91.0) | 60.0 (35.3-82.0) | 92.8 (74.7-113.0) | <0.001 | <0.001 | 85 (64.0-101.0) |
| VETC (N, %) | | | | <0.001 | <0.001 | |
| absence | 684 (68.2) | 558 (71.8) | 126 (55.8) | | | 15 (65.2) |
| presence | 319 (31.8) | 219 (28.2) | 100 (44.2) | | | 8 (34.8) |

Note: *, data are presented as mean±SD; #, data are presented as median and IQR ; ^, Adjusted P was

corrected using the Benjamini-Hochberg (FDR)

Abbreviations: FAP, fibroblast activation protein; HBV, hepatitis B virus; ALT, alanine aminotransferase; AST, aspartate aminotransferase; ALBI, albumin-bilirubin; AFP, alpha-fetoprotein; MVD, microvessel density; TLS, tertiary lymphoid structures VETC, vessels encapsulating tumor clusters;

*Histological staining analysis before and after matching between the low and high FAP expression groups*

The relationship between FAP expression levels and various clinicopathological features was evaluated in the retrospective cohort. Interreader agreement for the clinicopathological features was excellent (Kappa 0.84-0.91, Supplementary Table S2). Importantly, high FAP expression in HCC was significantly correlated with more aggressive clinicopathological characteristics (Table 1). Specifically, compared with low-FAP HCCs, high-FAP HCCs exhibited a significantly higher prevalence of poor tumor differentiation (51.3%, 116/226 vs. 30.8%, 239/777; adjusted P<0.001) and VETC patterns (44.2%,

100/226 vs. 28.2%, 219/777; adjusted P<0.001). Furthermore, high FAP expression was associated with increased MVD (92.8, IQR:74.7-113.0 vs. 60.0, IQR:35.3-82.0; adjusted P<0.001) and a lower presence of TLSs (39.4%, 89/226 vs. 54.8%, 426/777; adjusted P<0.001). To ensure the robustness of these findings, PSM and IPTW analyses were performed to eliminate baseline imbalances (Table 2). Following PSM (n=226 per group), high-FAP HCCs consistently demonstrated a significantly higher frequency of poor differentiation (51.3% vs. 32.7%, P<0.001), a higher prevalence of VETC patterns (44.2% vs. 28.3%, P=0.001), elevated MVD levels (P<0.001), and a reduced rate of intratumoral TLS (39.4% vs. 52.2%, P=0.008). These associations remained significant after IPTW analysis (low-FAP, n=1003; high-FAP, n=1000; all P < 0.05), further supporting the association between FAP expression and these pathological indicators.

Table 2. Baseline characteristics of the two groups after matching in retrospective cohort.

| Baseline characteristics | After PSM | | | | After IPTW | | | |
|---|---|---|---|---|---|---|---|---|
| | Low-FAP (n=226) | High-FAP (n=226) | *P* | *SMD* | Low-FAP (n=1003) | High-FAP (n=1000) | *P* | *SMD* |
| Age (years)* | 53.3±12.0 | 53.4±11.4 | 0.402 | 0.079 | 53.8±12.0 | 53.2±11.2 | 0.477 | 0.053 |
| Gender (N, %) | | | 0.798 | 0.036 | | | 0.550 | 0.046 |
| male | 188 (83.2) | 191 (84.5) | | | 840 (83.7) | 854 (85.4) | | |
| female | 38 (16.8) | 35 (15.5) | | | 163 (16.3) | 146 (14.6) | | |
| Underlying liver diseases (N, %) | | | 0.079 | 0.213 | | | 0.117 | 0.162 |
| absence | 37 (16.4) | 25 (11.1) | | | 139 (13.8) | 103 (10.3) | | |
| HBV | 165 (73.0) | 185 (81.9) | | | 773 (77.1) | 835 (83.5) | | |
| others | 24 (10.6) | 16 (7.1) | | | 91 (9.1) | 62 (6.2) | | |
| Liver cirrhosis (N, %) | | | 0.925 | 0.009 | | | 0.799 | 0.020 |
| absence | 120 (53.1) | 119 (52.7) | | | 511 (50.9) | 519 (51.9) | | |

| | | | | | | | | |
|---|---|---|---|---|---|---|---|---|
| presence | 106 (46.9) | 107 (47.3) | | | 492 (49.1) | 481 (48.1) | | |
| Ascites (N, %) | | | 0.116 | 0.163 | | | 0.399 | 0.066 |
| absence | 198 (87.6) | 209 (92.5) | | | 913 (91.3) | 928 (92.8) | | |
| little | 28 (12.4) | 17 (7.5) | | | 90 (8.7) | 72 (7.2) | | |
| Neutrophil ($\times10^9$) # | 3.60 (2.59-4.62) | 3.54 (2.44-4.64) | 0.694 | 0.030 | 3.27 (2.41-4.28) | 3.39 (2.33-4.27) | 0.834 | 0.002 |
| Lymphocyte ($\times10^9$) # | 1.39 (1.03-1.71) | 1.33 (1.03-1.65) | 0.608 | 0.087 | 1.38 (1.04-1.75) | 1.33 (1.03-1.66) | 0.332 | 0.099 |
| Platelet ($\times10^9$) # | 160 (121-211) | 162 (117-211) | 0.847 | 0.044 | 156 (110-209) | 157 (112-204) | 0.858 | 0.039 |
| Monocyte ($\times10^9$) # | 0.34 (0.26-0.47) | 0.36 (0.25-0.47) | 0.921 | 0.030 | 0.34 (0.25-0.46) | 0.34 (0.25, 0.45) | 0.713 | 0.080 |
| Albumin (g/L) # | 39.2 (36.5-42.2) | 39.2 (36.3-42.2) | 0.669 | 0.044 | 39.2 (36.3-42.1) | 39.3 (36.3-42.2) | 0.729 | 0.032 |
| Total bilirubin (umol/L) # | 13.7 (10.5-17.7) | 13.4 (9.9-19.0) | 0.901 | 0.168 | 13.8 (10.4-18.0) | 13.5 (9.9-19.1) | 0.965 | 0.204 |
| ALT (U/L) # | 28.7 (19.9-42.8) | 29.4 (19.8-45.7) | 0.990 | 0.101 | 31.2 (21.4-47.3) | 29.5 (19.9-46.0) | 0.272 | 0.022 |
| AST (U/L) # | 33.6 (24.7-49.7) | 33.6 (24.5-51.1) | 0.888 | 0.069 | 34.5 (24.8-49.8) | 33.2 (23.7-49.4) | 0.554 | 0.006 |
| Creatinine (umol/L) # | 71.2 (61.6-80.3) | 70.1 (59.6-79.9) | 0.560 | 0.005 | 71.5 (61.6-80.6) | 69.9 (59.6-79.9) | 0.410 | 0.003 |
| INR | 1.01 (0.96-1.08) | 1.03 (0.97-1.10) | 0.140 | 0.127 | 1.02 (0.96-1.09) | 1.02 (0.97-1.10) | 0.550 | 0.010 |

| | | | | | | | | |
|---|---|---|---|---|---|---|---|---|
| ALBI grade (N, %) | | | 0.571 | 0.062 | | | 0.122 | 0.120 |
| I | 108 (47.8) | 101 (44.7) | | | 503 (50.2) | 442 (44.2) | | |
| II | 118 (52.2) | 125 (55.3) | | | 500 (49.8) | 558 (55.8) | | |
| AFP (ng/mL, N, %) | | | 0.777 | 0.036 | | | 0.857 | 0.014 |
| ≤200 | 120 (53.1) | 124 (54.9) | | | 612 (61.0) | 604 (60.4) | | |
| >200 | 106 (46.9) | 102 (45.1) | | | 391 (39.0) | 396 (39.6) | | |
| Tumor size (mm, N, %) | | | 0.705 | 0.045 | | | 0.950 | 0.005 |
| ≤50 | 103 (45.6) | 98 (43.4) | | | 529 (52.7) | 525 (52.5) | | |
| >50 | 123 (54.4) | 128 (56.6) | | | 474 (47.3) | 475 (47.5) | | |
| Microvascular invasion (N, %) | | | 0.935 | 0.035 | | | 0.864 | 0.042 |
| absence | 159 (70.4) | 166 (70.8) | | | 742 (73.9) | 473 (47.3) | | |
| presence | 67 (29.6) | 66 (29.2) | | | 261 (26.1) | 527 (52.7) | | |
| Satellite lesions (N, %) | | | 0.837 | 0.029 | | | 0.690 | 0.030 |
| absence | 166 (70.8) | 157 (69.5) | | | 733 (73.0) | 717 (71.7) | | |
| presence | 66 (29.2) | 69 (30.5) | | | 270 (27.0) | 283 (28.3) | | |
| Tumor differentiation (N, %) | | | <0.001 | 0.383 | | | <0.001 | 0.392 |
| Moderately to well | 152 (67.3) | 110 (48.7) | | | 691 (68.9) | 500 (50.0) | | |
| poorly | 74 (32.7) | 116 (51.3) | | | 312 (31.1) | 500 (50.0) | | |
| Intratumoral TLS | | | 0.008 | 0.260 | | | 0.001 | 0.258 |
| absence | 108 (47.8) | 137 (60.6) | | | 456 (45.5) | 582 (58.2) | | |
| presence | 118 (52.2) | 89 (39.4) | | | 547 (54.5) | 418 (41.8) | | |

| | | | | | | | | | |
|---|---|---|---|---|---|---|---|---|---|
| MVD | 59.0 (33.2-80.7) | 92.8 (74.7-113.0) | <0.001 | 1.141 | 58.9 (34.7-81.4) | 94.5 (75.5-113.7) | <0.001 | 1.177 |
| VETC (N, %) | | | 0.001 | 0.336 | | | <0.001 | 0.308 |
| absence | 162 (71.7) | 126 (55.8) | | | 716 (71.4) | 568 (56.8) | | |
| presence | 64 (28.3) | 100 (44.2) | | | 287 (28.6) | 432 (43.2) | | |

Note: *, data are presented as mean±SD; #, data are presented as median and IQR

Abbreviations: FAP, fibroblast activation protein; HCC, hepatocellular carcinoma; PSM, propensity score matching; IPTW, Inverse Probability of Treatment Weighting; HBV, hepatitis B virus; ALBI, albumin-bilirubin; ALT, alanine aminotransferase; AST, aspartate aminotransferase; AFP, alpha-fetoprotein; ALBI, albumin-bilirubin; MVD, microvessel density; TLS, tertiary lymphoid structures VETC, vessels encapsulating tumor clusters

*Prognosis before and after matching between the low and high FAP expression groups*

The median follow-up time was 49.0 months (IQR: 27.5-71.9 months). By the end of the follow-up period, 482 patients had died (48.1%, 482/1003), and 668 had experienced tumor recurrence (66.6%, 668/1003). The median OS was 76.5 months ([95% CI: 66.8-86.2 months]), and the 1-, 2-, 3-, 4-, and 5-year OS rates were 89.8%, 78.8%, 70.2%, 63.1%, and 55.9%, respectively. The median RFS was 35.2 months ([95% CI: 30.4-40.1 months]), and the corresponding 1-, 2-, 3-, 4-, and 5-year RFS rates were 73.4%, 58.8%, 49.7%, 41.9%, and 35.8%, respectively (Table 3).

Before matching, patients in the low-FAP group had significantly better OS than those in the high FAP group (81.8 months, 95%CI: 70.8-97.3 months vs. 56.6 months, 95%CI: 46.4-65.3 months; P<0.001) and significantly longer RFS (40.6 months, 95%CI: 34.8-47.0 months vs. 20.5 months, 95%CI: 17.6-30.0 months; P<0.001) (Figure 4A-B). The post-adjustment survival analysis further supported the

prognostic relevance of FAP expression. After PSM, 226 matched pairs were generated, and no significant differences in baseline characteristics were observed between the two groups. The post-PSM analysis revealed that patients in the low-FAP group had significantly better OS (77.7 months [95%CI: 65.6-98.2 months] vs. 56.6 months [95%CI: 46.4-65.3 months]; P=0.041) and RFS (28.5 months [95%CI: 25.1-39.0 months] vs. 20.5 months [95%CI: 17.6-30.0 months]; P=0.023) than those in the high-FAP group (Figure 4C-D). For the IPTW analysis, weighted pseudo-cohorts comprising 1003 weighted patients in the low-FAP group and 1000 weighted patients in the high-FAP group were generated. After matching, patients with low-FAP HCCs maintained a significantly better OS (81.7 months [95%CI: 69.4-96.4 months] vs. 59.0 months [95%CI: 51.9-80.7 months]; P=0.030) and RFS (39.5 months [95%CI: 33.6-45.6 months] vs. 23.6 months [95%CI: 19.0-36.8 months]; P=0.021), compared to patients with high-FAP HCCs (Figure 4E-F). The RFS and OS between the Low FAP group and the High FAP groups before and after matching are summarized in Table 3.

Table 3. The RFS and OS between the Low FAP group and High FAP group before and after matching.

| | Entire population | Before matching | | | After PSM | | | After IPTW | | |
|---|---|---|---|---|---|---|---|---|---|---|
| | | Low FAP group (n=777) | High FAP group (n=226) | P | Low FAP group (n=226) | High FAP group (n=226) | P | Low FAP group (n=1003) | High FAP group (n=1000) | P |
| Median OS (95% | 76.5 (66.8-86.2) | 81.8 (70.8-97.3) | 56.6 (46.4-65.3) | <0.001 | 77.7 (65.6-98.2) | 56.6 (46.4-65.3) | 0.041 | 81.7 (69.4-96.4) | 59.0 (51.9-80.7) | 0.030 |

| | | | | | | | | | |
|---|---|---|---|---|---|---|---|---|---|
| CI) | | | | | | | | | |
| 1-year (%) | 89.8 | 91.1 | 85.0 | | 86.7 | 85.0 | | 90.8 | 86.2 |
| 2-year (%) | 78.8 | 80.9 | 71.1 | | 76.4 | 71.1 | | 80.3 | 73.3 |
| 3-year (%) | 70.2 | 72.3 | 62.6 | | 68.1 | 62.6 | | 71.6 | 65.8 |
| 4-year (%) | 63.1 | 65.4 | 54.6 | | 62.3 | 54.6 | | 64.6 | 57.4 |
| 5-year (%) | 55.9 | 58.3 | 46.6 | | 56.7 | 46.6 | | 57.6 | 49.0 |
| Median RFS (95% CI) | 35.2 (30.4-40.1) | 40.6 (34.8-47.0) | 20.5 (17.6–30.0) | <0.001 | 28.5 (25.1-39.0) | 20.5 (17.6–30.0) | 0.023 | 39.5 (33.6-45.6) | 23.6 (19.0-36.8) | 0.021 |
| 1-year | 73.4 | 75.8 | 65.0 | | 71.2 | 65.0 | | 75.0 | 68.1 |

| | | | | | | | |
|---|---|---|---|---|---|---|---|
| (%) | | | | | | | |
| 2-year (%) | 58.8 | 62.3 | 46.0 | 56.6 | 46.0 | 61.5 | 48.8 |
| 3-year (%) | 49.7 | 52.5 | 39.8 | 44.1 | 39.8 | 51.8 | 43.1 |
| 4-year (%) | 41.9 | 44.7 | 32.3 | 38.2 | 32.3 | 44.2 | 34.6 |
| 5-year (%) | 35.8 | 38.5 | 26.4 | 36.1 | 26.4 | 38.0 | 27.9 |

Abbreviations: RFS, Recurrence-free survival; OS, overall survival; HCC, hepatocellular carcinoma; PSM, propensity score matching; IPTW, inverse probability of treatment weighting.

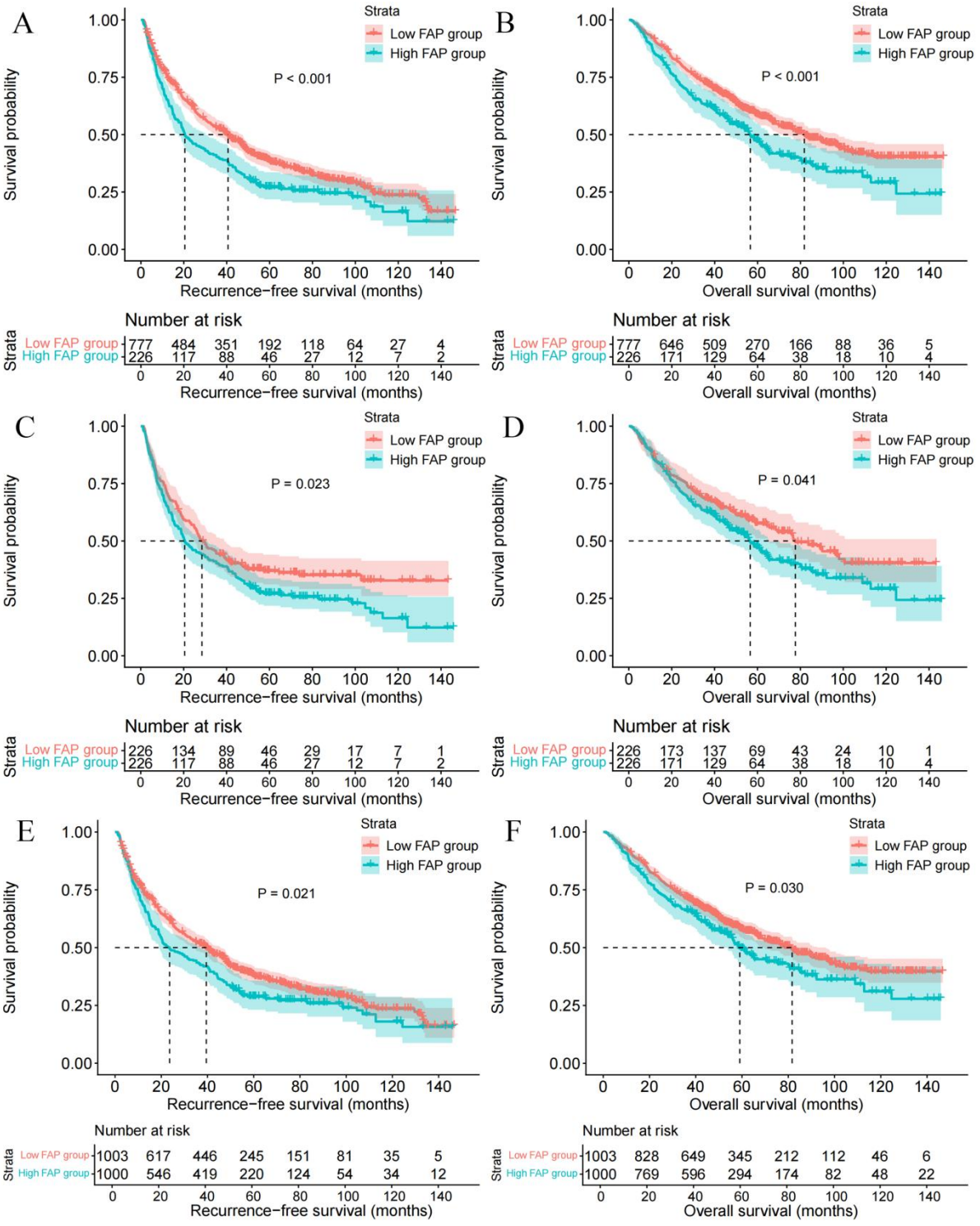



Figure 4. Survival curves for patients with Low FAP and High FAP HCCs before and after matching. RFS (A) and OS (B) before matching. RFS (C) and OS (D) after PSM analysis. RFS (E) and OS (F) after IPTW analysis. Before matching, both RFS and OS were significantly better for patients with low FAP HCCs than for those with high FAP HCCs. After PSM, patients with low FAP HCCs maintained a significantly

better RFS and OS, compared to patients with high FAP HCCs. In terms of IPTW analysis, patients with low FAP HCCs also had a better RFS and OS compared to patients with high FAP HCCs. FAP, fibroblast activation protein; HCC, hepatocellular carcinoma; OS, overall survival; RFS, recurrence-free survival; PSM, propensity score matching; IPTW, inverse probability of treatment weighting

*Independent prognostic value of FAP expression for RFS and OS*

Multivariable Cox proportional hazards regression analysis was performed in the entire cohort to simultaneously adjust for relevant clinical and pathological confounders (Table 4). Notably, to optimize model stability and represent the overall aggressive behavior of tumors, microvascular invasion and satellite lesions were combined and analyzed as "mVI/S,", which defined as positive if either situation was present. After fully controlling for variables such as age, tumor size, AFP, VETC, and TLS status, high FAP expression was successfully confirmed as an outstanding and independent adverse prognostic factor for both reduced RFS (Adjusted HR=1.21, 95% CI: 1.01-1.45, P=0.040) and worse OS (Adjusted HR=1.26, 95% CI: 1.02-1.55, P=0.033). In addition, liver cirrhosis, tumor burden beyond the up-to-seven criteria, larger tumor size, higher AFP levels, pathological high-risk invasive factors, and VETC positivity were identified as independent risk factors (Table 4).

Table 4. Multivariable Cox Proportional Hazards Analysis of Predictors for Recurrence-Free Survival and Overall Survival

| Variable | RFS | | | OS | | |
|---|---|---|---|---|---|---|
| | HR | 95% CI | P | HR | 95% CI | P |
| Age | 1.00 | 0.99-1.00 | 0.500 | 1.00 | 0.99-1.01 | 0.523 |
| Gender (N, %) | | | | | | |
| male | 1.00 | | | 1.00 | | |
| female | 0.93 | 0.75-1.15 | 0.498 | 0.95 | 0.74-1.22 | 0.710 |
| Underlying liver diseases (N, %) | | | | | | |
| absence | 1.00 | | | 1.00 | | |

| | | | | | | |
|---|---|---|---|---|---|---|
| HBV | 1.13 | 0.88-1.44 | 0.333 | 1.10 | 0.82-1.47 | 0.520 |
| others | 1.27 | 0.91-1.79 | 0.164 | 1.34 | 0.91-1.97 | 0.133 |
| Liver cirrhosis (N, %) | | | | | | |
| absence | 1.00 | | | 1.00 | | |
| presence | 1.21 | 1.04-1.41 | 0.015 | 1.26 | 1.05-1.52 | 0.012 |
| Up to seven criteria (N, %) | | | | | | |
| within | 1.00 | | | 1.00 | | |
| beyond | 1.53 | 1.31-1.80 | <0.001 | 1.81 | 1.50-2.18 | <0.001 |
| AFP level (N, %) | | | | | | |
| ⩽200 | 1.00 | | | 1.00 | | |
| >200 | 1.15 | 0.98-1.35 | 0.095 | 1.31 | 1.09-1.58 | 0.005 |
| TLS (N, %) | | | | | | |
| absence | 1.00 | | | 1.00 | | |
| presence | 0.89 | 0.76-1.04 | 0.135 | 0.93 | 0.77-1.12 | 0.458 |
| Tumor differentiation (N, %) | | | | | | |
| Moderately to well | 1.00 | | | 1.00 | | |
| poorly | 1.31 | 1.08-1.58 | 0.005 | 1.15 | 0.98-1.35 | 0.094 |
| mVI/S (N, %) | | | | | | |
| absence | 1.00 | | | 1.00 | | |
| presence | 1.45 | 1.24-1.69 | <0.001 | 1.28 | 1.07-1.54 | 0.008 |
| ALBI (N, %) | | | | | | |
| I | 1.00 | | | 1.00 | | |

| | | | | | | |
|---|---|---|---|---|---|---|
| II | 1.16 | 0.99-1.35 | 0.065 | 1.25 | 1.04-1.50 | 0.016 |
| VETC (N, %) | | | | | | |
| absence | 1.00 | | | 1.00 | | |
| presence | 1.27 | 1.08-1.50 | 0.004 | 1.25 | 1.04-1.52 | 0.020 |
| FAP level (N, %) | | | | | | |
| Low | 1.00 | | | 1.00 | | |
| High | 1.21 | 1.01-1.45 | 0.040 | 1.26 | 1.02-1.55 | 0.033 |

Abbreviations: HBV, hepatitis B virus; AFP, alpha-fetoprotein; TLS, tertiary lymphoid structures; VETC, vessels encapsulating tumor clusters; FAP, fibroblast activation protein

*Gene testing cohort for analysis of angiogenesis-related genes and immune infiltration levels*

To further examine the relationship between FAP expression levels, angiogenesis, and immune cell infiltration, 209910 single cells from 23 participants (high-FAP group, n=7; low-FAP group, n=16) in the prospective genomic-test cohort were analyzed. Unsupervised dimensionality reduction and clustering of the entire dataset identified 15 major cell lineages (Figure 5A). Given the pivotal role of T cells in the TME, the T-cell population was further re-clustered into distinct functional subsets (Figure 5B). Notably, higher FAP expression was positively correlated with *PDGFRB* expression (P<0.001, adjusted P<0.001) (Figure 5C) and was associated with reduced proportions of CD8+ tissue-resident memory T cells (TRM) (P=0.006, adjusted P=0.044) (Figure 5D). Functional enrichment analysis and GSEA were performed to explore the biological significance of high FAP expression. As shown in the bubble plot, high FAP expression was significantly associated with several oncogenic and stroma-remodeling pathways, including the MAPK, Wnt, and TGF-beta signaling pathways (Figure 5E). GSEA further showed that the high FAP group was enriched for gene sets associated with intratumoral angiogenesis and extracellular matrix (ECM) remodeling, including the VEGF signaling pathway (ES=0.5160, NP=0.0576), focal adhesion (ES=0.5171, NP=0.0087), and ECM-receptor interactions (Figure 5F-H). Furthermore, enrichment of the chemokine and T-cell receptor signaling pathways was consistent with an association between high FAP levels and a complex, potentially immunosuppressive TME.

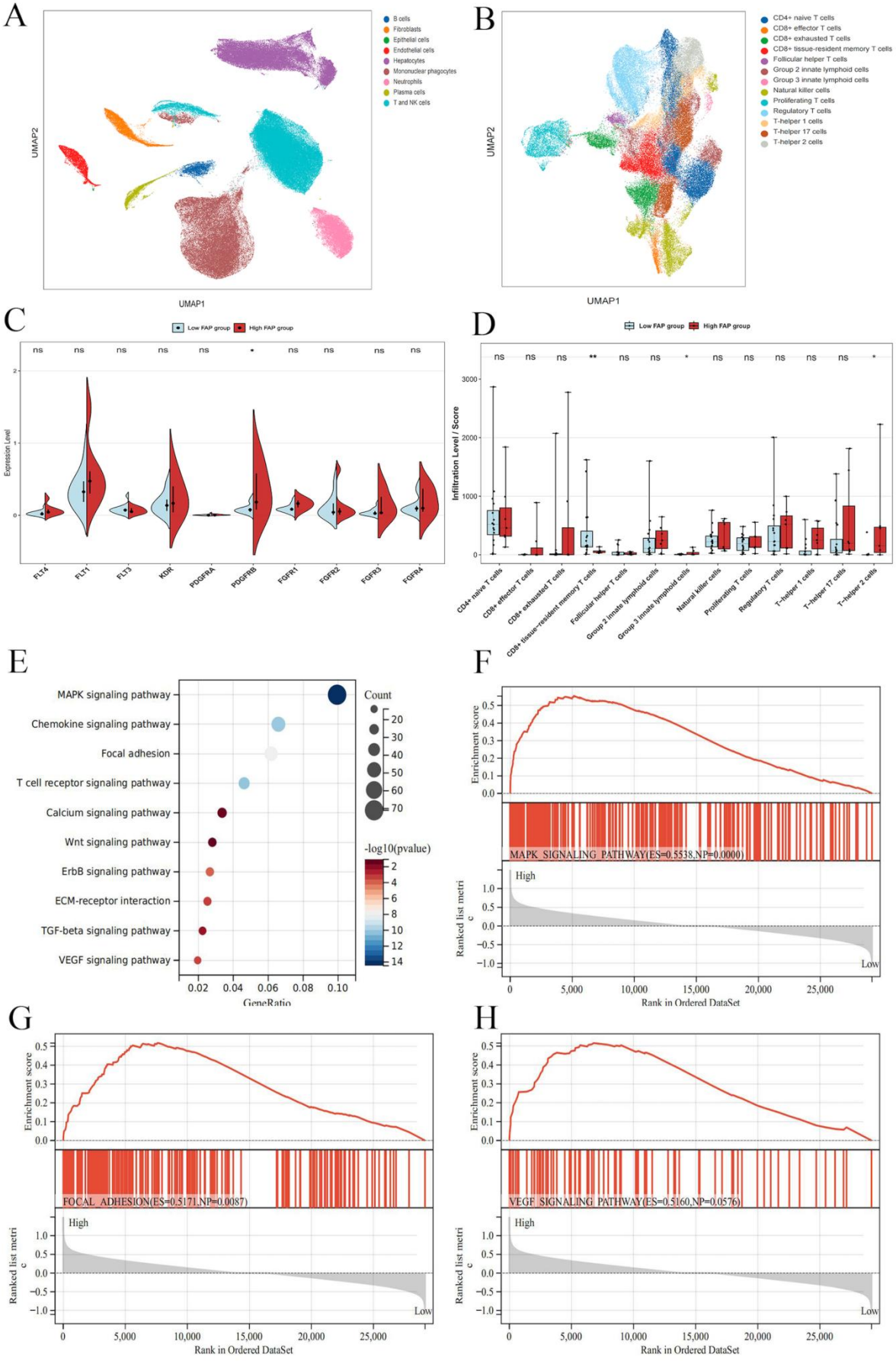

A
UMAP2
UMAP1
B cells
Fibroblasts
Epithelial cells
Endothelial cells
Hepatocytes
Mononuclear phagocytes
Neutrophils
Plasma cells
T and NK cells
B
UMAP2
UMAP1
CD4+ naive T cells
CD8+ effector T cells
CD8+ exhausted T cells
CD8+ tissue-resident memory T cells
Follicular helper T cells
Group 2 innate lymphoid cells
Group 3 innate lymphoid cells
Natural killer cells
Proliferating T cells
Regulatory T cells
T-helper 1 cells
T-helper 17 cells
T-helper 2 cells
C
Low FAP group
High FAP group
Expression Level
FLT4
FLT1
FLT3
KDR
PDGFRA
PDGFRB
FGFR1
FGFR2
FGFR3
FGFR4
D
Low FAP group
High FAP group
Infiltration Level / Score
CD4+ naive T cells
CD8+ effector T cells
CD8+ exhausted T cells
CD8+ tissue-resident memory T cells
Follicular helper T cells
Group 2 innate lymphoid cells
Group 3 innate lymphoid cells
Natural killer cells
Proliferating T cells
Regulatory T cells
T-helper 1 cells
T-helper 17 cells
T-helper 2 cells
E
MAPK signaling pathway
Chemokine signaling pathway
Focal adhesion
T cell receptor signaling pathway
Calcium signaling pathway
Wnt signaling pathway
ErbB signaling pathway
ECM-receptor interaction
TGF-beta signaling pathway
VEGF signaling pathway
Count
-log10(pvalue)
GeneRatio
F
Enrichment score
MAPK_SIGNALING_PATHWAY(ES=0.5538,NP=0.0000)
Ranked list metric
High
Low
Rank in Ordered DataSet
G
Enrichment score
FOCAL_ADHESION(ES=0.5171,NP=0.0087)
Ranked list metric
High
Low
Rank in Ordered DataSet
H
Enrichment score
VEGF_SIGNALING_PATHWAY(ES=0.5160,NP=0.0576)
Ranked list metric
High
Low
Rank in Ordered DataSet

Figure 5. Single-cell transcriptomic landscape and functional enrichment analyses based on FAP expression. (A) UMAP plot illustrating the 15 major cell lineages identified across the entire prospective scRNA-seq cohort (n=23). (B) UMAP plot showing the refined subclustering and annotation of T-cell subpopulations. (C) Violin plots comparing the expression levels of key angiogenesis-related genes between the high- and low-FAP expression groups. (D) Box plots showing the infiltration levels and proportions of distinct T-cell subsets between the high- and low-FAP groups. (E) Dot plot illustrating the differential enrichment of key signaling pathways involved in immune regulation and angiogenesis between the high- and low-FAP expression cohorts. GSEA plots showing the significant enrichment of the (F) MAPK, (G) FOCAL ADHESION, and (H) VEGF signaling pathways in the high FAP group compared to the low FAP group. Statistical significance was defined as follows: *, adjusted $P < 0.05$; **, adjusted $P < 0.01$; and ns, not significant (adjusted $P > 0.05$). FAP, fibroblast activation protein; GSEA, Gene Set Enrichment Analysis; UMAP, Uniform Manifold Approximation and Projection; ES, enrichment score; NP, nominal P-value.

## 4.Discussion

The biological heterogeneity of the TME is increasingly recognized as a major determinant of therapeutic failure in HCC [21]. In this study, we systematically analyzed a large multicenter cohort and found that high FAP expression was an independent prognostic marker of poor OS and RFS. Moreover, high FAP expression was associated with a proangiogenic and immunosuppressive microenvironment characterized by increased MVD count, enrichment of the VETC vascular pattern, and reduced formation of intratumoral TLSs. These observations suggest that FAP-positive CAFs may contribute to vascular remodeling and immune organization within the HCC microenvironment.

A key finding of our study was the positive correlation between FAP expression and the VETC pattern. VETC has been reported to facilitate the release of intact tumor clusters into the circulation, bypassing the need for cell-EMT (Epithelial-mesenchymal transition) and thereby enhancing metastatic efficiency [12]. Our data showed that high-FAP tumors exhibited significantly higher MVD and a greater prevalence of the VETC pattern. The scRNA-seq analysis further showed that elevated FAP levels were associated with enrichment of proangiogenic pathways, such as VEGF and MAPK signaling pathways. Furthermore, *PDGFRB* expression was significantly higher in the high-FAP group. These findings are consistent with a potential association between FAP-positive fibroblasts, endothelial organization, and ECM remodeling in tumors with VETC features. In addition, enrichment of the focal adhesion and ECM-receptor interaction pathways suggest that FAP-associated stromal remodeling may contribute to alterations in tumor vascular architecture, which may be related to the shorter RFS observed in patients with high FAP expression.

Another important finding of this study was that high FAP expression was negatively correlated with antitumor immune markers. High-FAP HCCs exhibited markedly lower rates of TLS and reduced proportions of CD8+ TRM. TLS are essential ectopic sites for lymphocyte recruitment and activation, and their absence or reduced abundance is often associated with "immunologically cold" tumors [22-23]. Our finding that high FAP expression correlated with lower TLS rates (39.4% vs. 54.8%) suggests that FAP-associated stromal remodeling may contribute to physical barriers that limit lymphocyte

infiltration and the formation of organized immune niches. Enrichment of the TGF-beta signaling pathway in high-FAP tumors further supports a possible association between FAP+ CAFs and restricted immune aggregate maturation. Furthermore, the reduced proportion of CD8+ TRM cells, which play a critical role in long-term immune surveillance and prevention against tumor recurrence [24-25], may partially explain the poorer postoperative prognosis observed in patients with high FAP expression.

The clinical implications of these findings suggest that FAP expression may help refine patient stratification for systemic therapy. Currently, combination therapy with antiangiogenic agents and immune checkpoint inhibitors is the standard first-line treatment for advanced HCC [26-27]. However, our data indicate that high-FAP expression may be associated with a less favorable response to ICIs, potentially related to the "immune-excluded" and "high-VETC" features. In this context, targeting FAP-positive fibroblasts may offer a complementary approach for modulating the TME. Recent studies have highlighted that 68Ga-FAPI PET/CT offers superior diagnostic sensitivity for HCC compared to traditional 18F-FDG [28], while pilot trials of 177Lu-FAPI radioligand therapy have demonstrated favorable safety profiles and promising tumor uptake [29,30]. Future studies should evaluate whether FAP-directed interventions can modify VETC-associated tumor dissemination and stromal barriers, and thereby improve responses to concurrent immunotherapy.

Several limitations of this study should be acknowledged. First, the sample size of the prospective genomic cohort was relatively small. Specifically, the high-FAP group included only seven of the 23 patients analyzed by scRNA-seq. Consequently, these single-cell transcriptomic findings should be considered exploratory rather than confirmatory. Furthermore, the association between high FAP expression and reduced CD8+ TRM cell exclusion showed only borderline statistical significance, warranting validation in larger, independent prospective trials. Second, although the multicenter retrospective design provided a large sample size, it could not completely eliminate the possibility of residual selection bias. Furthermore, our cohort predominantly comprised patients with HBV-related HCC, which may limit the generalizability of these FAP-centric immune exclusion patterns to Western populations, where MASLD- or HCV-related HCC is more frequent. Finally, the assessment of VETC

patterns and TLS relied on morphological evaluation, which may introduce interobserver variability despite the excellent interreader agreement observed in this study. Therefore, future studies should incorporate standardized digital pathology approaches to improve the reproducibility of these histopathological assessments.

In conclusion, our multicenter study identified FAP expression as an independent marker associated with a proangiogenic and immunosuppressive TME in HCC, characterized by enrichment of the VETC patterns and reduced intratumoral TLS formation. These findings suggest that FAP may contribute to the spatial organization of the tumor microenvironment and support further investigation of FAP-targeted interventions as a promising component of future combination therapeutic strategies aimed at overcoming treatment resistance and improving survival in patients with HCC.

List of abbreviations: HCC, Hepatocellular carcinoma; TME, Tumor microenvironment; CAFs, Cancer-associated fibroblasts; FAP, Fibroblast activation protein; ECM, Extracellular matrix; VETC, Vessels encapsulating tumor clusters; EMT, Epithelial-mesenchymal transition; TLS, tertiary lymphoid structures; LRE, liver Resection; INR, International normalized ratio; AFP, alpha-fetoprotein; CT, Computed tomography; MRI, Magnetic resonance imaging; OS, overall survival; RFS, Recurrence-free survival; PSM, Propensity score matching; IPTW, inverse probability of treatment weighting

**Declarations**

Ethics approval and consent to participate: This study was legally initiated and approved by the Medical Ethics Committee of the Second Xiangya Hospital of Central South University (the primary coordinating center; Approval No. Z0633-01), which covered both the retrospective cohort and the prospective genomic-test cohort. All experiments were performed in accordance with relevant guidelines and regulations, including the Declaration of Helsinki. Regarding informed consent, written

informed consent to participate was obtained from all participants in the prospective cohort (all recruited from the Second Xiangya Hospital). For the retrospective multi-institutional cohort, the study protocol and the waiver of written informed consent were fully reviewed and endorsed by the Medical Ethics Committees of all three participating centers (the Second Xiangya Hospital of Central South University, the Fourth Medical Center of PLA General Hospital, and Hunan Provincial Hospital of Integrated Traditional Chinese and Western Medicine) in accordance with local institutional guidelines.

Consent for publication: Not applicable.

Availability of data and materials: The single-cell RNA sequencing datasets generated during the current study are available in the NCBI BioProject repository under accession number PRJNA1482913 (https://www.ncbi.nlm.nih.gov/bioproject/PRJNA1482913).

Competing interests: The authors declare that they have no competing interests.

Funding: This study was supported by the Postgraduate Research Innovative Project of Central South University (No. 2026ZZTS0115)

Authors' contributions: Sang ZJ and Bao Y collected and provided the patients' clinical information, analyzed the clinical data. Sang ZJ drafted the manuscript. Lu WQ performed the histological slide review, edited and critically revised the manuscript for important intellectual content. Lu WQ acted as the lead contributor and serves as the guarantor of this work. All authors have read and approved the final version of the manuscript.

Acknowledgements: Not applicable.

**References:**

1. Vogel A, Meyer T, Sapisochin G, Salem R, Saborowski A. Hepatocellular carcinoma. Lancet. 2022;400(10360):1345-1362.
2. Wang TC, Wei N, Bao Y, et al. CT Radiomics-based Machine Learning to Identify Intratumoral Fibrosis and Underlying Angiogenesis in Hepatocellular Carcinoma. Radiology.

2026;319(2):e250736. doi:10.1148/radiol.250736.

3. Sung H, Ferlay J, Siegel RL, et al. Global Cancer Statistics 2020: GLOBOCAN Estimates of Incidence and Mortality Worldwide for 36 Cancers in 185 Countries. CA Cancer J Clin. 2021;71(3):209-249.
4. Reig M, Forner A, Rimola J, et al. BCLC strategy for prognosis prediction and treatment recommendation: The 2022 update. J Hepatol. 2022;76(3):681-693.
5. Llovet JM, Castet F, Heikenwalder M, et al. Immunotherapies for hepatocellular carcinoma. Nat Rev Clin Oncol. 2022;19(3):151-172.
6. Zhang K, He K, Zhang L, et al. Gadoxetic Acid-enhanced MRI Scoring Model to Predict Pathologic Features of Hepatocellular Carcinoma. Radiology. 2025;314(2):e233229. doi:10.1148/radiol.233229.
7. Sahai E, Astsaturov I, Cukierman E, et al. A framework for advancing our understanding of cancer-associated fibroblasts. Nat Rev Cancer. 2020;20(3):174-186.
8. Kraman M, Bambrough PJ, Arnold JN, et al. Suppression of antitumor immunity by stromal cells expressing fibroblast activation protein-alpha. Science. 2010;330(6005):827-830.
9. Wang TC, Huang W, Li SX, et al. High Fibroblast Activation Protein Expression in Hepatocellular Carcinoma: CT Imaging Features and Histological Characteristics. Acad Radiol. 2025;32(9):5137-5149. doi:10.1016/j.acra.2025.04.016.
10. Puré E, Blomberg R. Pro-tumorigenic roles of fibroblast activation protein in cancer: back to the basics. Oncogene. 2018;37(32):4343-4357.
11. Fang JH, Zhou HC, Zhang C, et al. A novel vascular pattern promotes metastasis of hepatocellular carcinoma in an epithelial-mesenchymal transition-independent manner. Hepatology. 2015;62(2):452-465.
12. Huang BY, Mi ZQ, Zhang XY, et al. Vessels encapsulating tumor clusters promote noninvasive metastasis of hepatocellular carcinoma by shaping an immunosuppressive microenvironment. J Clin Invest. 2026;136(4):e193758.
13. Zhu Y, Wang M, Cao J, Song H, Zhang P. Vessels encapsulating tumor clusters in hepatocellular

carcinoma: a distinct metastatic pathway with diagnostic and therapeutic significance. J Transl Med. 2026;24(1):185.

14. Calderaro J, Petitprez F, Becht E, et al. Intra-tumoral tertiary lymphoid structures are associated with a low risk of early recurrence of hepatocellular carcinoma. J Hepatol. 2019;70(1):58-65.
15. Sautès-Fridman C, Petitprez F, Calderaro J, Fridman WH. Tertiary lymphoid structures in the era of cancer immunotherapy. Nat Rev Cancer. 2019;19(6):307-325.
16. Kalluri R. The biology and function of fibroblasts in cancer. Nat Rev Cancer. 2016;16(9):582-598.
17. Mariathasan S, Turley SJ, Nickles D, et al. TGF $\beta$ attenuates tumour response to PD-L1 blockade by contributing to exclusion of T cells. Nature. 2018;554(7693):544-548.
18. Torbenson MSNI, Park YN, Roncalli M, Sakamoto M. WHO classification of tumors series. 5th ed. Lyon, France: International Agency for Research on Cancer, 2019; 229-239.
19. Dziadek S, Kraxner A, Cheng WY, et al. Comprehensive analysis of fibroblast activation protein expression across 23 tumor indications: insights for biomarker development in cancer immunotherapies. Front Immunol. 2024;15:1352615.
20. Liu ZL, Chen HH, Zheng LL, Sun LP, Shi L. Angiogenic signaling pathways and anti-angiogenic therapy for cancer. Signal Transduct Target Ther. 2023;8(1):198.
21. Donne R, Lujambio A. The liver cancer immune microenvironment: Therapeutic implications for hepatocellular carcinoma. Hepatology. 2023;77(5):1773-1796.
22. Yuan X, Xiao Y, Yu D. Turn cold tumors hot by reprogramming the tumor microenvironment. Nat Biotechnol. 2025;43(4):466-470.
23. Zhao R, Gao D. Innate Immunity and Tertiary Lymphoid Structures. Immunol Rev. 2025;332(1):e70052.
24. Virassamy B, Caramia F, Savas P, et al. Intratumoral CD8+ T cells with a tissue-resident memory phenotype mediate local immunity and immune checkpoint responses in breast cancer. Cancer Cell. 2023;41(3):585-601.e8.
25. Corgnac S, Boutet M, Kfoury M, Naltet C, Mami-Chouaib F. The Emerging Role of CD8+ Tissue

Resident Memory T (TRM) Cells in Antitumor Immunity: A Unique Functional Contribution of the CD103 Integrin. Front Immunol. 2018;9:1904.

26. Finn RS, Qin S, Ikeda M, et al. Atezolizumab plus Bevacizumab in Unresectable Hepatocellular Carcinoma. N Engl J Med. 2020;382(20):1894-1905.
27. Matuschewski NJ, Sobirey R, Revzin M, et al. Noninvasive Tumor Profiling: Quantitative Contrast-Enhanced MRI Markers Predict PD-L1 and CTNNB1 Status in Hepatocellular Carcinoma. Radiology. 2025;316(2):e242750. doi:10.1148/radiol.242750.
28. Wang H, Zhu W, Ren S, et al. 68Ga-FAPI-04 Versus 18F-FDG PET/CT in the Detection of Hepatocellular Carcinoma. Front Oncol. 2021;11:693640.
29. Liu H, Guo R, Zhang X, et al. Safety and efficacy of 177Lu-FAPI-XT radioligand therapy in patients with advanced sarcoma and other cancer entities: first-in-human, dose-escalation study. Eur J Nucl Med Mol Imaging. 2026;53(3):1869-1880.
30. Al-Ibraheem A, Abdlkadir AS, Ruzzeh S, et al. [177Lu]Lu-FAPI Radioligand Therapy: Emerging Horizons and Clinical Promise in Solid Tumors: A Comprehensive Review. Semin Nucl Med.

## Supplementary Files

This is a list of supplementary files associated with this preprint. Click to download.

- Table1.docx
- Table3.docx
- Table2.docx
- Table4.docx
- Supplementarymaterials.pdf